

Decay spectroscopy of the blocked fission product ^{130}I A. Mattera^{1,*}, E. A. McCutchan^{1,†}, S. Zhu^{1,‡}, C. Morse¹, M. P. Carpenter², P. Copp², C. Müller-Gatermann², W. Reviol², J. P. Greene² and M. Gott²¹National Nuclear Data Center, Brookhaven National Laboratory, Upton, New York 11973-5000, USA²Physics Division, Argonne National Laboratory, Lemont, Illinois 60439, USA

(Received 31 May 2022; revised 25 July 2022; accepted 12 December 2022; published 26 December 2022)

Numerous applications rely on the identification and quantification of fission products with the activation technique, where γ rays emitted in the decay are used to estimate the initial activity of the radionuclide of interest. ^{130}I is a so-called *blocked* fission product, which can be produced only directly through fission, a property that makes it particularly attractive for nuclear forensics. A source of ^{130}I was produced using a (p, n) reaction on enriched ^{130}Te at the Brookhaven Tandem Van de Graaff, and its decay was studied with the Gammasphere at Argonne National Laboratory. Two new levels were identified, and over 25 transitions were added, removed, or replaced in the level scheme with intensity measurements made down to $I_\gamma = 0.00066$ per 100 decays. The uncertainty on the intensities of the strongest transitions, those that are commonly used to quantify the activity of the radionuclide, was improved by a factor of 2 compared to the previous best assessment, and discrepancies in the literature values were resolved. A detailed angular correlation analysis further permitted the determination of a number of spin assignments for excited levels and mixing ratios for γ -ray transitions.

DOI: [10.1103/PhysRevC.106.064326](https://doi.org/10.1103/PhysRevC.106.064326)

I. INTRODUCTION

^{130}I was used in the early years of radiation therapy as an isotope to cure certain endocrinological diseases [1]. Although its use in radiation therapy was later abandoned in favor of ^{131}I , more abundantly produced in nuclear fission, ^{130}I has found utility in other applications relating to nuclear forensics and the nuclear fuel cycle. The neighbor to ^{130}I , ^{129}I , is a long-lived fission product that can be released into the environment at the end of the nuclear fuel cycle. The long half-life of ^{129}I ($T_{1/2}$ on the order of 10^7 yr [2,3]) and the single γ -ray emission of only 39.6 keV, makes it a long-term radiological hazard which is difficult to quantify. The experimental challenge of measuring ^{129}I decay is circumvented by producing ^{130}I through neutron activation analysis (NAA) and measuring its strong γ -ray emissions. NAA on ^{129}I and the subsequent measurement of ^{130}I β decay, has been shown to be a convenient technique to ascertain the amount of ^{129}I in various samples [4–6].

^{130}I exhibits additional properties which make it attractive for use in nuclear forensics [8]. As shown in Fig. 1, ^{130}I is a so-called “blocked fission fragment” i.e., because of the very long-lived ($Z - 1$) isobar ^{130}Te ($T_{1/2}$ on the order of 10^{20} yr [9,10]), its production in fission can only happen directly and not through decay of more neutron-rich nuclides. Following a nuclear event, a cumulative fission yield is generally measured, which is the sum of the direct yield from fission, and

the contribution from all the fission products that eventually β decay into the measured isotope. It is well known that the direct yield of fission products changes with the fissioning system (fissile isotope and excitation energy), and whereas this propagates somewhat to the cumulative yields, the interpretation of this dependence can be less straightforward because the original yield information often becomes muted due to the feeding from the more neutron-rich precursors. For long-lived *blocked* products, the direct yield can be measured hours or days after the initial fission event. This property makes ^{130}I particularly enticing for nuclear forensics as measuring the amount of ^{130}I relative to other well-known fission products can provide valuable information about the initial fission event that produced it [8].

Despite its importance, the evaluated data [9] on ^{130}I almost entirely stems from a single measurement by Hopke *et al.* [11], performed in 1973 with two HPGe detectors. More recent works by Musthafa *et al.* [12] and by Sakharov [13] reported the intensity of a few strong transitions following ^{130}I decay. These differ from those of Hopke *et al.* [11] by up to 30%, even for the most intense transitions.

In order to provide a solid foundation of γ -ray intensities for the use of ^{130}I in applications, we revisit the decay of the ground state of ^{130}I ($T_{1/2} = 12.36(1)$ h [9]) using the Gammasphere array [14] to obtain the most complete picture of the β decay of ^{130}I to date. In particular, we confirm much of the level scheme proposed by Hopke *et al.* [11] and newly identify or replace more than 25 transitions. Using the 4π -angular coverage of the Gammasphere, we were also able to measure angular correlations for a number of transitions, which allowed us to unambiguously make spin assignments to several levels. Finally, the disagreement between the γ -ray

*amattera@bnl.gov

†mccutchan@bnl.gov

‡Deceased.

¹³² Ba >3.0E+21yr 2e	¹³³ Ba 10.551yr ε=100.00%	¹³⁴ Ba STABLE 2.417%	¹³⁵ Ba STABLE 6.592%	¹³⁶ Ba STABLE 7.854%	¹³⁷ Ba STABLE 11.232%	¹³⁸ Ba STABLE 71.698%
¹³¹ Cs 9.689d ε=100.00%	¹³² Cs 6.480d ε=99.13% β=1.87%	¹³³ Cs STABLE 100%	¹³⁴ Cs 2.0652yr β=100.00% ε=3.0E-4%	¹³⁵ Cs 3.3E+6y β=100.00%	¹³⁶ Cs 13.04d β=100.00%	¹³⁷ Cs 30.08yr β=100.00%
¹³⁰ Xe STABLE 4.0710%	¹³¹ Xe STABLE 21.232%	¹³² Xe STABLE 26.9086%	¹³³ Xe 5.2475d β=100.00%	¹³⁴ Xe >5.8E+22yr 10.4357% 2β ⁻	¹³⁵ Xe 9.14h β=100.00%	¹³⁶ Xe >2.4E+21yr 8.8573% 2β ⁻
¹²⁹ I 1.57E+7y β=100.00%	¹³⁰ I 12.36h β=100.00%	¹³¹ I 8.0252d β=100.00%	¹³² I 2.295h β=100.00%	¹³³ I 20.83h β=100.00%	¹³⁴ I 52.5m β=100.00%	¹³⁵ I 6.58h β=100.00%
¹²⁸ Te 2.41E+24yr 31.74% 2β=100.00%	¹²⁹ Te 69.9m β=100.00%	¹³⁰ Te ε=3.0E+24yr 34.03% 2β=100.00%	¹³¹ Te 25.0m β=100.00%	¹³² Te 3.204d β=100.00%	¹³³ Te 12.5m β=100.00%	¹³⁴ Te 41.8m β=100.00%

FIG. 1. Portion of the chart of nuclides around the *blocked* fragment ¹³⁰I: because of the long half-life of ¹³⁰Te, production of this fission product in a nuclear event can only happen directly through fission, and not via β⁻ decay of a precursor. Other *blocked* fragments, ¹³⁴Cs and ¹³⁶Cs, are also circled [7].

intensities reported in the various works was settled, often in favor of the adopted values originally measured by Hopke *et al.* [11].

II. THE EXPERIMENT

A source experiment to study the decay of ¹³⁰I into ¹³⁰Xe was conducted at Argonne National Laboratory (ANL) using the Gammasphere array [14]. The ¹³⁰I source was produced via the (*p*, *n*) reaction on a stack of isotopically pure ¹³⁰Te foils (total thickness ≈6.2 mg/cm²). The foils were manufactured at the Center for Accelerator Target Service, Physics Division, ANL, evaporating 99.5% ¹³⁰Te on a 40 μg/cm² carbon substrate. The irradiation was performed at the Brookhaven Tandem Van de Graaff facility [15], Brookhaven National Laboratory, where a 7.5-MeV proton beam at a current of 125 pA was delivered on the stack for 8.5 h. At the end of the irradiation, the stack was packaged and shipped to ANL where it was installed in the center of the Gammasphere, approximately 30 h after the end of beam with an estimated source strength of ≈11 μCi.

For this paper the Gammasphere array consisted of 49 Compton-suppressed HPGe detectors placed in 15 angular rings around the array's symmetry axis; the array has nominally 17 such rings, and the symmetry axis coincides with the beam axis in an accelerator experiment. Data were collected with a digital data-acquisition system selecting all multiplicity ≥1 singles triggers for approximately 28 h; 2.9 × 10⁹ single γ-ray events and 6 × 10⁸ γ-γ coincident events were collected on disk. Data were sorted with the GSSORT package [16] into singles histograms and γ-γ coincidence matrices. The singles spectrum of the β decay of ¹³⁰I is shown in Fig. 2(a). Since the daughter of ¹³⁰I, ¹³⁰Xe, is stable, and thanks to the target purity and the reaction used to produce the sources, no other long-lived isotopes were observed in the spectra. The quality of the coincidence spectra are demonstrated in Fig. 2(b) with a gate on the 536-keV 2⁺ → 0⁺ transition.

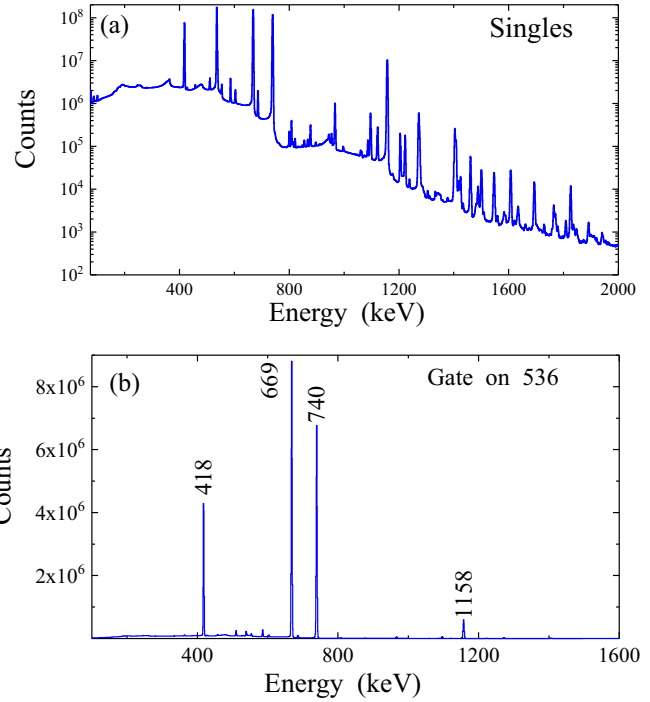


FIG. 2. (a) Singles spectrum and (b) spectrum gated on the 536-keV transition following the decay of ¹³⁰I. Peaks are labeled by their energy in keV.

Data analysis was performed with the RADWARE package [17], GF3M, modified for matrix analysis.

Energy and efficiency calibrations were performed using well-characterized transitions in the decay of ¹⁵²Eu [19], ⁵⁶Co [20], ¹⁸²Ta [21], and ²⁴³Am [22]. A 0.08-keV systematic uncertainty was estimated and added in quadrature to the statistical uncertainty in the energy determination, whereas an additional 1.4% uncertainty was applied to all measured intensities to account for the systematic uncertainty in the efficiency calibration.

As precise intensity measurements were an essential component of this paper, they were determined in two ways. When the transitions were isolated peaks, confirmed through the γ-γ matrix, the intensities were first obtained from the singles spectrum. In addition, intensities were determined for all transitions from the γ-γ matrix. This was accomplished by placing a gate on a transition depopulating a level, and determining the area of a transition feeding into the same level. The intensities were deduced from the area, corrected for the detector efficiencies, and the branching ratio of the depopulating transition. Details of this procedure can be found in Ref. [23]. In cases where both a singles and a γ-γ determination of the intensity could be performed, the quoted result is a weighted average of the two measurements.

A γ-γ angular correlation analysis was performed for pairs of transitions where statistics were sufficient. Data were sorted according to certain relative angles θ between the Gamma-sphere rings. In particular, 12 angle pair combinations were considered, corresponding to θ = 21°, 35°, 41°, 53°, 55°, 61°, 67°, 71°, 73°, 75°, 79°, and 87°. The efficiency of each angle

bin was determined by finding the number of counts in each peak corresponding to the cascade pair and comparing it to the total number of counts in each peak in the singles spectrum. The normalized intensity distribution as a function of these angles yielded the angular correlation between transitions γ_1 and γ_2 . The angular correlations were fit with the standard expansion in Legendre polynomials.

III. EXPERIMENTAL RESULTS

The energies and intensities of the γ rays assigned to the decay of ^{130}I in the present work as well as the corresponding states and their quantum numbers are given in Table I. All intensities were normalized relative to the strongest transition in the level scheme, taking $I_\gamma(536 \text{ keV}) = 100$. Intensities from the present paper are compared to those in the adopted data [9], showing overall good agreement. Level energies given in Table I are derived from a least-squares fit to all measured γ -ray energies. The present analysis allowed us to identify two new levels as being populated in the β decay of ^{130}I . The high-statistics data and the γ - γ coincidence capabilities allowed us to add, remove, or replace more than 25 transitions with respect to those previously assigned to the decay of ^{130}I by Hopke *et al.* [11]. The levels populated in ^{130}Xe and their γ decay led to the level scheme in Fig. 3.

A. Decay scheme construction

The present paper finds good agreement with the level scheme previously proposed by Hopke *et al.* [11]. All excited levels are confirmed, and we identify two new levels populated in the β decay of ^{130}I at 2298.7 and 2615.3 keV. These new levels decay by two and four newly identified γ -ray transitions, respectively. Overall, we identify, remove or replace over 25 new transitions which connect the excited levels. In the following discussion, we give a few example spectra to illustrate the level of statistics available to identify new transitions and justify our removal of previously placed transitions.

A level at 2362 keV was proposed by Hopke *et al.* [11], on the basis of seven depopulating transitions. In the present paper, we confirm and measure the intensity for five of the seven transitions previously reported. The 190-keV transition could not be isolated, and our upper limit is less stringent than the one proposed by Hopke *et al.* [11]. The previously proposed 730-keV transition would feed into the 1633-keV level. Gated spectra on the 511- and 1097-keV transitions depopulating the 1633-keV level lack evidence for a transition of 730 keV as shown in Fig. 4. A 730-keV transition was observed in the spectra gated on the 1546- and 877-keV transitions as shown in Fig. 5 which from coincidence relations and energy sums, places the 730-keV transition as depopulating a previously identified level at 2812 keV. In the present paper, the intensity of the 730-keV transition is determined as 0.0031(4), considerably smaller than the intensity determined by Hopke *et al.* [11], $I_\gamma = 0.011(8)$, although statistically compatible because of the significant uncertainty on the latter.

Hopke *et al.* [11] proposed a level at 2706 keV, based on two depopulating transitions. In the present paper, we con-

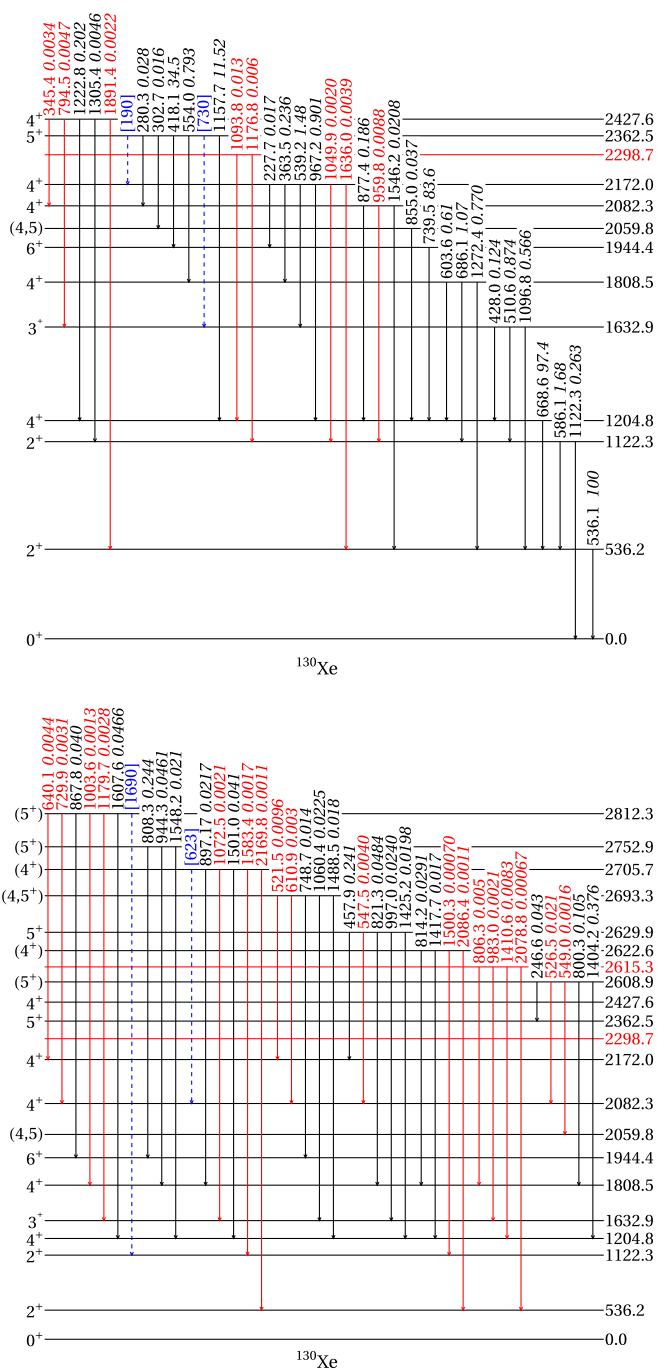


FIG. 3. Levels in ^{130}Xe populated in the β decay of ^{130}I . Transitions are labeled by their energy in keV, followed by their intensity in italics. New levels/transitions are highlighted in red. Previously reported transitions not confirmed in this paper are marked in blue. Figure created with SciDraw [18].

firm the 897-keV depopulating transition with an intensity in excellent agreement with the previous measurement. We find no evidence for the 623-keV transition, which would populate the 2082-keV level. Gated spectra on the 1546- and 877-keV transitions depopulating the 2082-keV level show no evidence for a 623-keV transition as shown in Fig. 5. In addition, we observe three new transitions depopulating the

TABLE I. Levels populated in the decay of ^{130}I to ^{130}Xe and their γ -ray decays. The relative intensities for γ -ray transitions are given by I_γ . The intensities are normalized to $I_\gamma(536\text{ keV}) = 100$. The intensities are also compared with those from Hopke *et al.* [11]. J^π assignments from the evaluated data [9] except where indicated. Multipolarities and mixing ratios are based on an angular correlation analysis and decay patterns, see the text and Table II. Assumed multipolarities are given in square brackets. For some cases, the angular correlation analysis provided more than one solution for δ . The δ value corresponding to the lowest χ^2 is given here whereas Table II provides both solutions for δ when applicable.

J_i^π	E_i (keV)	J_f^π	E_f (keV)	E_γ (keV)	I_γ	Mult.	δ	I_γ^{lit} [11]
2^+	536.16(7)	0^+	0.00	536.14(8)	100.0(14)	$E2$		100
2^+	1122.32(7)	2^+	536.16	586.11(9)	1.68(3)	$M1 + E2$	+6.2(10)	1.71(6)
		0^+	0.00	1122.34(10)	0.263(7)	$E2$		0.256(11)
4^+	1204.80(8)	2^+	536.16	668.62(8)	97.4(14)	$E2$		97(3)
3^+	1632.89(8)	4^+	1204.80	428.05(12)	0.124(9)	$M1 + E2$	-0.24(2)	0.084(11) ^h
		2^+	1122.32	510.57(8)	0.874(15)	$[M1 + E2]$		0.86(3)
		2^+	536.16	1096.75(10)	0.566(20)	$M1 + E2$	+0.81(11)	0.558(20)
$4^{\text{+d}}$	1808.52(9)	4^+	1204.80	603.62(11)	0.61(1)	$M1 + E2$	+0.67(2)	0.62(3)
		2^+	1122.32	686.10(9)	1.07(2)	$E2$		1.08(4)
		2^+	536.16	1272.42(22)	0.770(15)	$E2$		0.756(25)
6^+	1944.43(9)	4^+	1204.80	739.52(8)	83.6(13)	$E2$		83(3)
$(4,5)^e$	2059.80(14)	4^+	1204.80	854.96(15)	0.037(1)	+0.22(4)($J=5$), +0.34(6)($J=4$)		0.035(5)
$4^{\text{+d}}$	2082.29(9)	4^+	1204.80	877.44(11)	0.186(4)	$M1 + E2$	+0.10(5)	0.193(10)
		2^+	1122.32	959.8(2) ^a	0.0088(5)	$[E2]$		
		2^+	536.16	1546.2(2)	0.0208(18)	$[E2]$		0.023(4)
$4^{\text{+f}}$	2172.02(9)	6^+	1944.43	227.7(2)	0.017(3)	$[E2]$		0.012(5)
		4^+	1808.52	363.5(2)	0.236(15)	$M1 + E2$	+0.56(8)	0.09(2)
		3^+	1632.89	539.15(15)	1.48(5)	$M1 + E2$	+0.26(1)	1.41(4)
		4^+	1204.80	967.16(9)	0.901(25)	$M1(+E2)$	-0.01(3)	0.89(3)
		2^+	1122.32	1049.9(2) ^a	0.0020(4)	$[E2]$		
		2^+	536.16	1636.0(2) ^a	0.0039(5)	$[E2]$		
	2298.72(16) ^b	4^+	1204.80	1093.81(15) ^a	0.013(2)			0.028(8)
		2^+	1122.32	1176.8(3) ^a	0.006(2)			
5^+	2362.49(9)	4^+	2172.02	[190] ^c	<0.002			<0.0005
		4^+	2082.29	280.26(12)	0.028(3)	$[M1 + E2]$		0.024(7)
		$(4,5)$	2059.80	302.7(3)	0.016(3)			0.013(5)
		6^+	1944.43	418.06(9)	34.5(5)	$M1 + E2$	-0.43(2)	34.5(10)
		4^+	1808.52	553.96(11)	0.793(23)	$M1 + E2$	+0.29(3)	0.67(3)
		3^+	1632.89	[730] ^c	<0.0004			0.011(8)
		4^+	1204.80	1157.72(9)	11.52(18)	$M1 + E2$	+0.28(1)	11.4(4)
$4^{\text{+d}}$	2427.64(10)	4^+	2082.29	345.45(15) ^a	0.0034(4)	$[M1 + E2]$		
		3^+	1632.89	794.5(2) ^a	0.0047(4)	$[M1 + E2]$		
		4^+	1204.80	1222.84(12)	0.202(6)	$M1 + E2$	+0.10(6)	0.181(8)
		2^+	1122.32	1305.4(2)	0.0046(4)	$[E2]$		0.0049(2)
		2^+	536.16	1891.4(2) ^a	0.0022(3)	$[E2]$		
$(5^+)^g$	2608.88(10)	5^+	2362.49	246.55(14)	0.043(3)	$[M1 + E2]$		0.047(5)
		4^+	2082.29	526.54(12) ^a	0.021(2)	$[M1 + E2]$		
		$(4,5)$	2059.80	549.0(2) ^a	0.0016(3)			
		4^+	1808.52	800.25(12)	0.105(4)	$M1 + E2$	+0.28(8)	0.102(5)
		4^+	1204.80	1404.15(15)	0.376(20)	$M1 + E2$	+0.31(3)	0.348(16)
	2615.25(21) ^b	4^+	1808.52	806.3(5) ^a	0.005(2)			
		3^+	1632.89	983.0(4) ^a	0.0021(5)			
		4^+	1204.80	1410.6(5) ^a	0.0083(10)			
		2^+	536.16	2078.8(3) ^a	0.00067(20)			
$(4^+)^g$	2622.61(11)	4^+	1808.52	814.17(15)	0.0291(9)	$(M1(+E2))$	-0.1(6)	0.025(5)
		4^+	1204.80	1417.73(15)	0.017(2)	$[M1 + E2]$		0.012(2)
		2^+	1122.32	1500.3(2) ^a	0.00070(25)	$[E2]$		
		2^+	536.16	2086.4(2) ^a	0.0011(2)	$[E2]$		
$5^{\text{+g}}$	2629.88(10)	4^+	2172.02	457.87(12)	0.241(10)	$[M1 + E2]$		0.239(15)
		4^+	2082.29	547.5(2) ^a	0.0040(4)	$[M1 + E2]$		
		4^+	1808.52	821.25(14)	0.0484(19)	$M1 + E2$	-0.42 ⁺¹⁰ ₋₁₃	0.043(5)
		3^+	1632.89	997.01(12)	0.0240(15)	$[E2]$		0.028(5)

TABLE I. (Continued.)

J_i^π	E_i (keV)	J_f^π	E_f (keV)	E_γ (keV)	I_γ	Mult.	δ	I_γ^{lit} [11]
(4, 5 ⁺) ^j	2693.28(11)	4 ⁺	1204.80	1425.16(12)	0.0198(13)	[M1 + E2]		0.021(2)
		4 ⁺	2172.02	521.50(15) ^a	0.0096(13)			
		4 ⁺	2082.29	610.87(12) ^a	0.0033(3)			
		6 ⁺	1944.43	748.7(2)	0.014(2)			0.012(5)
		3 ⁺	1632.89	1060.38(12)	0.0225(16)			0.017(5)
		4 ⁺	1204.80	1488.5(2)	0.018(2)			0.012(2)
(4 ⁺) ^g	2705.73(11)	2 ⁺	1122.32	[1570.7]	<0.0001 ⁱ			
		4 ⁺	2082.29	[623] ^c	<0.0007			0.017(11)
		4 ⁺	1808.52	897.17(12)	0.0217(18)	[M1(+E2)]	0.0(5)	0.021(5)
		3 ⁺	1632.89	1072.5(3) ^a	0.0021(6)	[M1 + E2]		
		4 ⁺	1204.80	1500.98(12)	0.041(3)	(M1 + E2)	+0.14(11)	0.040(2)
		2 ⁺	1122.32	1583.4(2) ^a	0.0017(5)	[E2]		
(5 ⁺) ^g	2752.88(10)	2 ⁺	536.16	2169.8(3) ^a	0.0011(2)	[E2]		
		6 ⁺	1944.43	808.34(10)	0.244(10)	[M1 + E2]		0.238(10)
		4 ⁺	1808.52	944.33(12)	0.0461(23)	(M1 + E2)	+0.3(2)	0.063(14)
		4 ⁺	1204.80	1548.24(12)	0.021(2)	(M1 + E2)	+0.23(13)	0.018(4)
(5 ⁺) ^g	2812.27(10)	4 ⁺	2172.02	640.14(15) ^a	0.0044(8)	[M1 + E2]		
		4 ⁺	2082.29	729.91(15) ^a	0.0031(4)	[M1 + E2]		
		6 ⁺	1944.43	867.76(10)	0.040(2)	[M1 + E2]		0.043(6)
		4 ⁺	1808.52	1003.6(3) ^a	0.0013(2)	[M1 + E2]		
		3 ⁺	1632.89	1179.7(3) ^a	0.0028(3)	[E2]		
		4 ⁺	1204.80	1607.64(12)	0.0466(22)	(M1 + E2)	-0.12(6)	0.045(3)
2 ⁺	1122.32	[1690]	<0.00016					

^aNewly observed γ -ray transition following the decay of ^{130}I .

^bNew level observed following the decay of ^{130}I .

^cTransition previously placed in the decay scheme of ^{130}I , however, the present experiment finds no evidence for.

^dTentative assignment in evaluated data [9] is consistent with present angular correlation results. Decay to 2⁺ and 4⁺ levels limits the J^π to 2⁺, 3, 4⁺. Angular correlation analysis for the decay to the 4⁺ 1204.8 level or the 4⁺ 1808.5 level favors 4 for the parent level, with a mixed $D + Q$ transition, further supporting the positive-parity assignment.

^eSee the text for a discussion on the spin assignment of this level.

^fDecay of this level to 2⁺ and 6⁺ levels suggests $J^\pi = 4^+$. This is further supported by the angular correlation analysis for the decay to the 4⁺ 1808.5 level which favors 4 for the parent level with a mixed $D + Q$ transition, in agreement with the positive parity assignment.

^gNew J^π assignment with J from present angular correlation measurement, decay pattern, and β feeding considerations with parity inferred also from decay pattern and the assumption that $D + Q$ transitions with nonzero value of the mixing ratio are $M1 + E2$ in character.

^hReported as a doublet by Hopke *et al.* [11], with a 427.93-keV transition with $I_\gamma = 0.84(11)$ from the 1633-keV level and a 429.12-keV transition with $I_\gamma = 0.34(11)$ with no placement in the level scheme.

ⁱRef. [24] places a 1570.7-keV transition as depopulating the 2693.3-keV level following the ε decay of ^{130}Ce . In the present paper, no evidence is found for such a transition.

^jDecay of this level to 3⁺ and 6⁺ levels tentatively suggests $J^\pi = (4^+, 5^+)$.

2706-keV level with energies of 1073, 1583, and 2170 keV. Support for the placement of the 1073-keV transition is given in Fig. 4 where the transition is observed in both the 511-keV and the 1097-keV gates, placing it as a transition feeding into the 1633-keV level. One final transition warrants some discussion, which is the 1500.98-keV transition. In Hopke *et al.* [11], this is placed in both their table and level scheme drawing as originating from the 2623-keV level. This placement does not agree with the coincidence relations provided in Hopke *et al.* [11], which show a 1502-keV transition in coincidence with the 536- and 668-keV transitions. These coincidences are in agreement with the present paper and the placement of the 1501-keV transition as depopulating the 2706-keV level. Note that the evaluated data [9] also give the 1501-keV transition as originating from the 2706-keV level, but with no explanation on why the placement differs from that of Hopke *et al.* [11]. Interestingly, we do observe a much

weaker 1500.3-keV transition as depopulating the 2623-keV level.

A level at 2812 keV was proposed by Hopke *et al.* [11] based on three depopulating transitions, 868, 1608, and 1690 keV which decay into the 6₁⁺, 4₁⁺, and 2₂⁺ levels, respectively. We confirm the 868- and 1608-keV transitions with intensities in excellent agreement with Ref. [11]. No evidence is found for the 1690-keV transition populating the 2₂⁺ level at 1122 keV as shown in Fig. 6. Clearly observed in Fig. 6 are three additional transitions with intensities comparable or smaller than the reported intensity of the 1690-keV transition.

Finally, Hopke *et al.* [11] assign five additional transitions to the decay of ^{130}I at 158.8, 293.5, 429.1, 771.0, and 1094.3 keV without being able to place them in the decay scheme. The present data find no evidence for the first four transitions in either the singles or coincidence spectra, whereas the last one could correspond to the

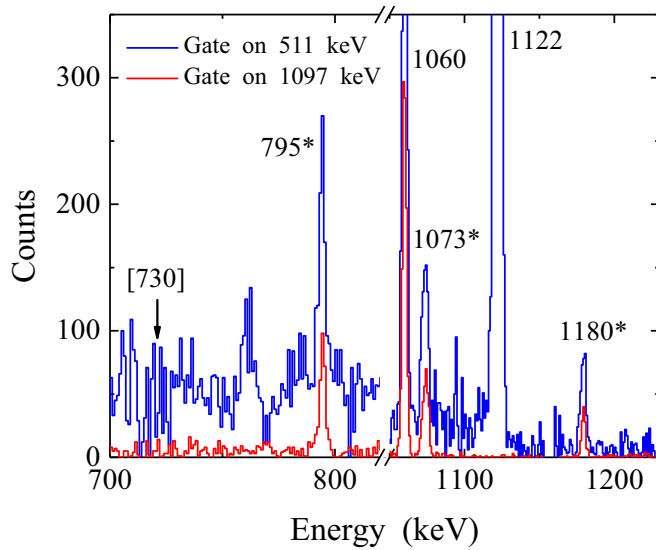


FIG. 4. Spectra gated on the 511-keV transition (blue line) and 1097-keV transition (red line). γ -ray transitions are labeled by their energy in keV; an asterisk indicates newly observed transitions, whereas the unobserved 730-keV transition is shown in brackets. Note the cut in the x -axis scale between 850 and 1050 keV.

1093.8-keV transition depopulating the newly proposed level at 2298.7 keV.

B. Spin and parity assignments

The spins of the low-lying levels in ^{130}Xe are well known [9], which allows one component of the cascade in the γ - γ angular correlation to be constrained. For most measurements, a gate on a well-established $E2$ transition was used to determine the character of the other transition in the cascade. As given

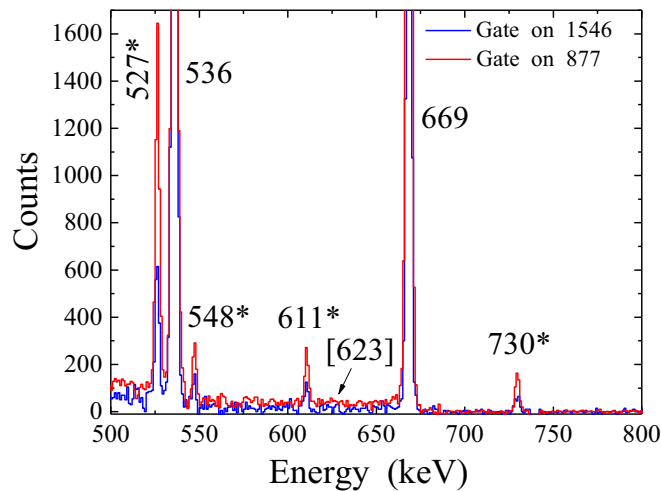


FIG. 5. Spectra gated on the 1546-keV transition (blue line) and 877-keV transition (red line). γ -ray transitions are labeled by their energy in keV; an asterisk indicates newly observed transitions, whereas a 623-keV transition is not observed and indicated by brackets.

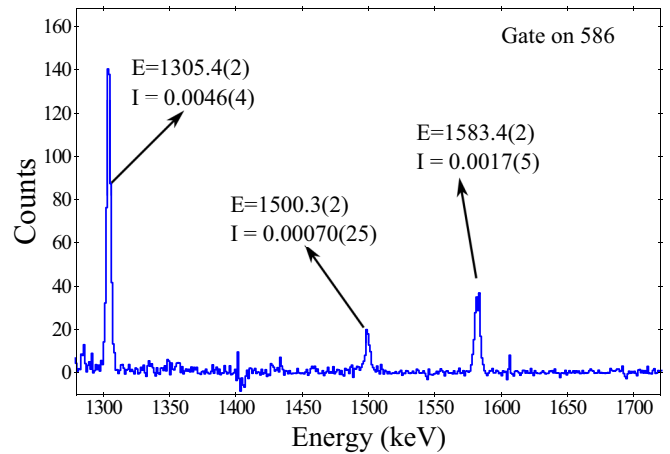


FIG. 6. Spectra gated on the 586-keV transition providing evidence for the nonobservation of a 1690-keV transition reported with $I_\gamma = 0.055(10)$. γ -ray transitions are labeled by energy in keV and intensity.

in Table II, gates were taken on the 536-keV $2_1^+ \rightarrow 0_1^+$, 669-keV $4_1^+ \rightarrow 2_1^+$, 1122-keV $2_2^+ \rightarrow 0_1^+$, 1272-keV $4_2^+ \rightarrow 2_1^+$, and 740-keV $6_1^+ \rightarrow 4_1^+$ transitions. The only exception is the 539–1097 keV cascade where the multipolarity and mixing ratio of the 1097-keV transition was fixed to the value obtained analyzing the gate on the 536-keV transition. In the fits, the spin of the initial level and multipolarity of the second transition in the cascade were allowed to vary. In varying the spin and multipolarity, we include the following constraints: (a) only $\Delta J \leq 2$ transitions were considered for the initial J , (b) for levels fed directly in the β decay of the $J^\pi = 5^+$ parent, the initial J was limited to 4–6 and (c) decay properties of other transitions depopulating the levels were taken into consideration. Condition (c) was generally manifested by excluding $J = 5$ for a level which decays to 2^+ levels. Condition (b) applies to levels above 2600 keV which are fed only in the β -decay process with no γ -ray feeding observed from higher-lying levels. Out of these levels for which we had sufficient statistics to perform the angular correlation analysis, the β -decay feeding ranges from approximately 0.05% to 0.5%. Even with feeding of a few tenths of a percent, at this high excitation energy the corresponding $\log ft$ values are around 7.8, allowing for the spins of these levels to be constrained to $J = 4$ –6.

Results of the analysis are summarized in Table II. The data used to extract the values for the cascades, and the results of the fit are provided in the Supplemental Material [25]. Mixing ratios are given in the convention of Krane and Steffen [26] and uncertainties are determined at the 68% confidence level. In some instances, the angular correlation analysis results in two χ^2 minima for δ . Both solutions are given in column 7 of Table II, the first value corresponding to the lower χ^2 value. Although the angular correlations given D , Q , or $D + Q$ nature for the transitions, additional constraints on the electric/magnetic character can be performed with some physics assumptions. First we assume the $E2$ character for stretched Q transitions. Additionally, we assume $D + Q$ transitions with large nonzero mixing ratios to be $M1 + E2$ in

TABLE II. Results of the γ - γ angular correlation analysis for ^{130}Xe . Measured a_2 and a_4 coefficients are given for each analyzed cascade along with the deduced multipolarity and mixing ratio. E_{lev} and J_{init} are the initial level energy and spin of the cascade, respectively. For each cascade, γ_2 corresponds to a stretched Q transition except where noted. In some instances, the angular correlation analysis results in two χ^2 minima for δ . Both solutions are given in the δ_{γ_1} column with the first value corresponding to the lower χ^2 value. Mixing ratios are compared with the evaluated data [9] and more recent measurements of Refs. [24,27].

E_{lev}	J_{init}	$\gamma_1\gamma_2$ (keV)	a_2	a_4	Mult. $_{\gamma_1}$	δ_{γ_1}	δ [9]	δ [24]	δ [27]
1122.3	2	586-536	-0.180(20)	0.28(3)	$D + Q$	+6.2(10)	+3.75(12)	+4.4 $^{+6}_{-17}$	+4.41 $^{+42}_{-51}$, -0.160 $^{+18}_{-15}$
1204.8	4	669-536	0.102(1)	0.0081(8)	Q	0.0	0.0	0.0	0.0
1632.9	3	1097-536	0.277(11)	-0.017(16)	$D + Q$	+0.81(11)	+1.3 $^{+38}_{-8}$	+0.84 $^{+55}_{-36}$	+0.611 $^{+46}_{-41}$
1632.9	3	428-669	0.057(8)	-0.022(11)	$D + Q$	-0.24(2)		+0.19 $^{+47}_{-40}$	+3.0 $^{+15}_{-10}$, +0.51 $^{+17}_{-13}$
1808.5	4	1272-536	0.119(10)	0.015(14)	Q	0.0	0.0	0.0	0.0
1808.5	4	686-1122	0.098(22)	-0.04(3)	Q	0.0	0.0	0.0	0.0
1808.5	4	604-669	-0.036(7)	0.063(10)	$D + Q$	+0.67(2)			+2.4 $^{+13}_{-7}$ or -0.37 $^{+18}_{-20}$
1944.4	6	740-669	0.101(1)	0.0101(14)	Q	0.0	0.0	0.0	0.0
2059.8	4	855-669	0.069(23)	-0.02(3)	$D + Q$	+0.34(6)			
2059.8	5	855-669	0.069(23)	-0.02(3)	$D + Q$	+0.22(4)		-0.05(14)	
2082.3	4	877-669	0.164(16)	-0.012(23)	$D + Q$	+0.10(5)			
2172.0	4	967-669	0.201(9)	-0.039(12)	$D(+Q)$	-0.01(3) ^b			
2172.0	4	539-1097 ^a	0.148(11)	-0.007(16)	$D + Q$	+0.26(1)			
2172.0	4	364-1272	-0.05(3)	-0.10(4)	$D + Q$	+0.56(8) ^b			
2362.5	5	1158-669	0.102(3)	0.012(4)	$D + Q$	+0.28(1) ^b	+0.28(3)	2.3 $^{+11}_{-9}$	
2362.5	5	554-1272	0.108(16)	0.002(23)	$D + Q$	+0.29(3)			
2362.5	5	418-740	0.173(2)	0.000(2)	$D + Q$	-0.43(2) ^b	-0.42(3)	-0.54(20)	
2427.6	4	1223-669	0.165(21)	0.04(3)	$D + Q$	+0.10(6), 1.1(2) ^c			
2608.9	5	1404-669	0.115(16)	0.026(23)	$D + Q$	+0.31(3)			
2608.9	5	800-1272	0.10(4)	0.02(6)	$D + Q$	+0.28(8), +2.7(8)			
2622.6	4	814-1272	0.22(7)	-0.09(11)	$D(+Q)$	-0.1(6)			
2629.9	5	821-1272	-0.32(5)	-0.01(8)	$D + Q$	-0.42 $^{+10}_{-13}$, -3.1 $^{+9}_{-14}$ ^c			
2705.7	4	1501-669	0.15(4)	-0.01(6)	$D + Q$	+0.14(11), -1.1(5)			
2705.7	4	897-1272	0.18(12)	-0.18(17)	$D(+Q)$	0.0(5)			
2752.9	5	1548-669	0.07(7)	0.09(9)	$D + Q$	+0.23(13), +3.1 $^{+38}_{-14}$			
2752.9	5	944-1272	0.09(8)	0.08(11)	$D + Q$	+0.3(2), 2.8 $^{+23}_{-11}$			
2812.3	5	1608-669	-0.15(4)	-0.07(6)	$D + Q$	-0.12(6)			

^aAnalysis performed by fixing the mixing ratio of the 1097-keV transition in the cascade to $\delta = 0.81(11)$.

^bQuality of the fit is poor with χ^2 larger than ten at the minimum.

^cThe second solution for δ has a χ^2 which is comparable to that of the first solution.

character. Finally, in instances where the initial and final J^π 's could be determined, we applied that information to constrain the multipolarity.

Included in Table II are the mixing ratios from the latest evaluation [9] along with two recent measurements performed after the 2001 evaluation. In Ref. [24], ^{130}Xe was populated in the ε decay of ^{130}Cs , and an angular correlation analysis was performed. In Ref. [27], ^{130}Xe was studied using an $(n, n'\gamma)$ reaction and spins and mixing ratios determined using angular distribution measurements. Overall, we obtain excellent agreement with prior measurements. For example, for the strong 418–740 keV cascade, corresponding to a well established $J = 5$ -6-4 sequence, our value of $\delta = -0.43(2)$ is in excellent agreement with the adopted value of $-0.42(3)$ and the more recent measurement of $-0.54(20)$ [24].

In Fig. 7, we provide a few examples where our analysis differs from the results in the literature. The 428-keV, $3^+ \rightarrow 4^+$ transition was not measured at the time of the 2001 ENSDF evaluation [9]. Subsequently, a mixing ratio of $+0.19^{+47}_{-40}$ was determined in Ref. [24] and two solutions for δ obtained in Ref. [27], $+3.0^{+15}_{-10}$ or $+0.51^{+17}_{-13}$. The present analysis using

the 428-669, 3-4-2 cascade favors the smaller value for δ as shown in Fig. 7(a), yielding a δ value of $-0.24(2)$. For comparison, the solution with $\delta = +3$ is included, exhibiting a very different pattern to the measured intensities versus $\cos(\theta)$.

The 1158-keV, $5^+ \rightarrow 4^+$ transition has an adopted mixing ratio of $+0.28(3)$, however, a more recent measurement determined $\delta = +2.3^{+11}_{-9}$. The angular correlation of 1158 keV-669 keV, 5-4-2 cascade is given in Fig. 7(b). The present data are in excellent agreement with the adopted value of δ . Included in Fig. 7(b) is the $\delta = +2.3$ solution, which clearly is not consistent with the measured angular correlation.

Finally, the 2060-keV level has a single depopulating transition of 855 keV and assigned $J^\pi = (5)^-$ [9]. The basis for the J^π assignment is an $E1$ character for the 855-keV transition which was determined through a measurement of the $\alpha(K)$ value [28]. Additional support for a pure dipole transition comes from the angular correlation measurement of Ref. [24], which determined $\delta = -0.05(14)$. As shown in Fig. 7(c), the present angular correlation data favor a larger mixing ratio with similar χ^2 values of the fit obtained for $J =$

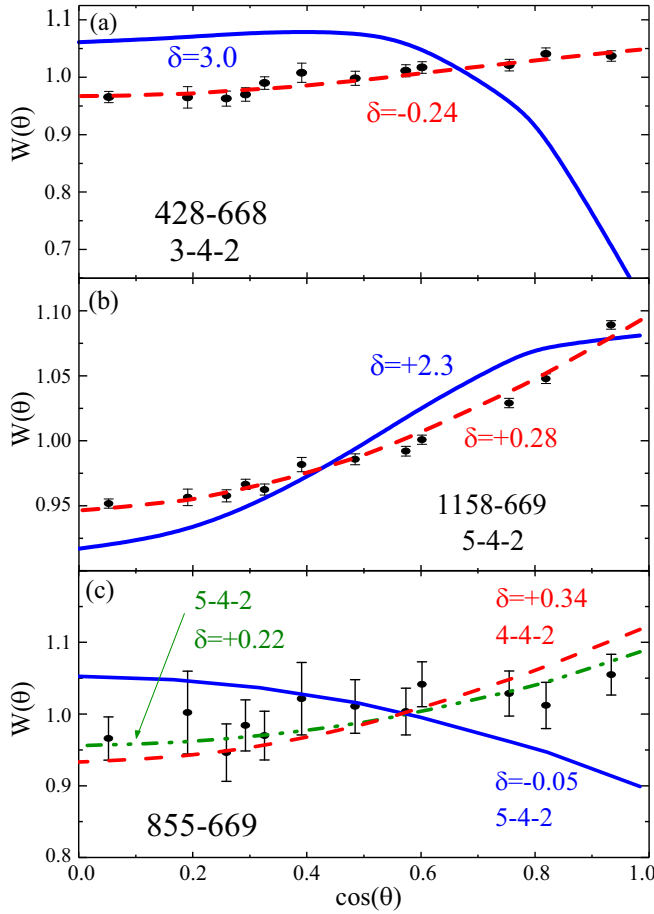


FIG. 7. Selected angular correlations analyzed following the decay of ^{130}I . Data are given by the solid circles whereas theoretical predictions by the lines with the mixing ratio indicated in the figure. Examples include the (a) 428–668-keV cascade, the (b) 1158–669-keV cascade, and the (c) 855–669-keV cascade.

4, $\delta = +0.22(4)$, and $J = 5$, $\delta = +0.34(6)$. Thus, the present experiment suggests J^π values of (4,5), which we tentatively assign given the discrepancy with previous measurements.

IV. DISCUSSION

Of direct interest for applications is the absolute intensities of the γ -ray transitions per 100 decays of ^{130}I . Negligible direct feeding of the ground state of ^{130}Xe is expected due to the highly forbidden β transition between the 5^+ ground state of ^{130}I and the 0^+ ground state of ^{130}Xe ($I_{\beta+\epsilon} < 10^{-8}$, $\log ft > 20$). Furthermore, with the data collected in this experiment it was possible to observe transitions more than five orders of magnitude weaker than the strongest $2^+ \rightarrow 0^+$ transition at 536.1 keV. These two aspects of the decay allow for the determination of the absolute intensity by summing all γ -ray intensities and conversion electrons directly feeding the ground state. From this, we deduce that the 536-keV γ ray is observed in 99.006(13)% of the decays. This is in agreement with the evaluated value of 99% [9] and provides an uncertainty which is essential for the use in applications.

TABLE III. Intensity [relative to $I_\gamma(536 \text{ keV}) = 100\%$] of the main γ -ray transitions measured by Hopke *et al.* [11], Musthafa *et al.* [12], and Sakharov [13].

E_γ (keV)	Hopke <i>et al.</i> [11]	Musthafa <i>et al.</i> [12]	Sakharov [13]	This paper
418.06	34.5(10)	33.4(39)	26.5(9)	34.5(5)
539.15	1.41(4)		1.19(6)	1.48(5)
586.11	1.71(6)		2.32(14)	1.68(3)
668.62	97(3)	92(11)	90(7)	97.4(14)
739.52	83(3)	79(9)	79(4)	83.6(13)
1157.72	11.4(4)	9.3(11)	8.2(6)	11.52(18)

A direct comparison of the intensities measured in the previous studies [11–13] is summarized in Table III. The intensities reported in the most recent measurements, which hinted at a disagreement with the values reported by Hopke *et al.* [11], were not confirmed in our paper. This is a particularly important result for applications as many of the transitions studied by Musthafa *et al.* [12] and Sakharov [13] were reported for the most intense transitions that would be more likely used in the identification and quantification of ^{130}I . In particular, for the transition at 739.5 keV, reported by Hopke *et al.* [11], Musthafa *et al.* [12], and Sakharov [13] as 83(3)%, 79(9)%, and 79(4)%, respectively, we not only essentially confirm the older results, but we reduce the uncertainty on the intensity by a factor of 2 on the most precise determination. A similar trend is observed for the transition at 668.6 keV, which Musthafa *et al.* [12] and Sakharov [13] report with an intensity of 92(11)% and 90(7)%, respectively and we measured as 97.4(14)% in agreement with Hopke’s value of 97(3)% [11]. Also for the 418.1-keV transition, reported by Musthafa *et al.* [12] and Sakharov [13] as 33.4(39) and 26.5(9), we found our result, 34.5(5)%, in good agreement with the one measured by Hopke *et al.* [34.5(10)] [11].

V. CONCLUSION

^{130}I is a *blocked* fission product of particular interest for nuclear forensics. Taking advantage of the sensitivity and granularity of the Gammasphere array, we provided the most complete description of the β^- decay of ^{130}I to date. We report the intensity for 70 transitions, over 25 of which were identified for the first time, or replaced in the level scheme using γ - γ coincidence data. The intensities of the strongest transitions, those that will be used in the quantification of this radionuclide in forensics application and measurements of fission yields with the activation technique, have been improved by a factor of 2 with respect to the best determination available until now. Finally, using the angular resolution of the Gammasphere, spin and parity assignments were provided for most levels using γ - γ angular correlation analysis.

ACKNOWLEDGMENTS

This work was supported by the U.S. Department of Energy, National Nuclear Security Administration, Office of

Defense Nuclear Nonproliferation Research and Development (DNN R&D), and by the Office of Nuclear Physics, Office of Science of the U.S. Department of Energy, under Contracts No. DE-AC02-98CH10886 (Brookhaven National Laboratory) and No. DE-AC02-06CH11357 (Argonne National

Laboratory). This research used resources of ATLAS-ANL, which is a DOE Office of Science User Facility. We acknowledge the staff at the Brookhaven Tandem Van de Graaff facility for their assistance during the irradiation.

-
- [1] S. Hertz and A. Roberts, *JAMA, J. Am. Med. Assoc.* **131**, 81 (1946).
- [2] J. Timar, Z. Elekes, and B. Singh, *Nucl. Data Sheets* **121**, 143 (2014).
- [3] E. García-Toraño, T. Altzitzoglou, P. Auerbach, M.-M. Bé, C. Bobin, P. Cassette, F. Chartier, R. Dersch, M. Fernández, H. Isnard *et al.*, *Appl. Radiat. Isot.* **140**, 157 (2018).
- [4] D. C. Aumann, H. Faleschini, and L. Friedmann, *Radiochim. Acta* **29**, 209 (1981).
- [5] J. H. Chao, C. L. Tseng, C. J. Lee, C. C. Hsia, and S. P. Teng, *Appl. Radiat. Isot.* **51**, 137 (1999).
- [6] X. Hou, *Radioact. Environ.* **11**, 371 (2008).
- [7] A. A. Sonzogni, in *International Conference on Nuclear Data for Science and Technology*, edited by R. C. Haight, M. B. Chadwick, T. Kawano, and P. Talou, AIP Conf. Proc. No. 769 (AIP, Melville, NY, 2005), pp. 574–577.
- [8] A. C. Hayes, *Rep. Prog. Phys.* **80**, 026301 (2017).
- [9] B. Singh, *Nucl. Data Sheets* **93**, 33 (2001).
- [10] A. Caminata, D. Adams, C. Alduino, K. Alfonso, F. Avignone, O. Azzolini, G. Bari, F. Bellini, G. Benato *et al.*, *Universe* **5**, 10 (2019).
- [11] P. K. Hopke, A. G. Jones, W. B. Walters, A. Prindle, and R. A. Meyer, *Phys. Rev. C* **8**, 745 (1973).
- [12] M. M. Musthafa, B. P. Singh, M. G. V. Sankaracharyulu, H. D. Bhardwaj, and R. Prasad, *Phys. Rev. C* **52**, 3174 (1995).
- [13] S. L. Sakharov, in *Proceedings of the 49th Meeting on Nuclear Spectroscopy and Nuclear Structure* (Dubna, Russia, 1999).
- [14] I.-Y. Lee, *Nucl. Phys. A* **520**, c641 (1990).
- [15] K. S. Smith, D. B. Steski, M. J. Zarccone, and P. Thieberger, in *Production and Neutralization of Negative Ions and Beams*, AIP Conf. Proc. No. 287 (AIP, Melville, NY, 1992), pp. 513–521.
- [16] The GSSort package, <http://www.phy.anl.gov/gammasphere/doc/index.html>, 2015.
- [17] D. C. Radford, *Nucl. Instrum. Methods Phys. Res., Sect. A* **361**, 297 (1995).
- [18] M. A. Caprio, *Comput. Phys. Commun.* **171**, 107 (2005).
- [19] M. J. Martin, *Nucl. Data Sheets* **114**, 1497 (2013).
- [20] H. Junde, H. Su, and Y. Dong, *Nucl. Data Sheets* **112**, 1513 (2011).
- [21] B. Singh, *Nucl. Data Sheets* **130**, 21 (2015).
- [22] C. D. Nesaraja and E. A. McCutchan, *Nucl. Data Sheets* **121**, 695 (2014).
- [23] M. A. Caprio, N. V. Zamfir, R. F. Casten, C. J. Barton, C. W. Beausang, J. R. Cooper, A. A. Hecht, R. Krucken, H. Newman, J. R. Novak *et al.*, *Phys. Rev. C* **66**, 054310 (2002).
- [24] L. Bettermann, C. Fransen, S. Heinze, J. Jolie, A. Linnemann, D. Mücher, W. Rother, T. Ahn, A. Costin, N. Pietralla *et al.*, *Phys. Rev. C* **79**, 034315 (2009).
- [25] See Supplemental Material at <http://link.aps.org/supplemental/10.1103/PhysRevC.106.064326> for the γ - γ angular correlation data and fit results.
- [26] K. S. Krane and R. M. Steffen, *Phys. Rev. C* **2**, 724 (1970).
- [27] E. E. Peters, T. J. Ross, S. F. Ashley, A. Chakraborty, B. P. Crider, M. D. Hennek, S. H. Liu, M. T. McEllistrem, S. Mukhopadhyay, F. M. Prados-Estévez *et al.*, *Phys. Rev. C* **94**, 024313 (2016).
- [28] L. Goettig, C. Droste, A. Dygo, T. Morek, J. Srebrny, R. Broda, J. Styczeń, J. Hattula, H. Helppi, and M. Jääskeläinen, *Nucl. Phys. A* **357**, 109 (1981).